

# Integrated Fluid-Thermal-Structural Analysis Using 6-node Triangular Finite Element Method and Adaptive Meshing Technique

Niphon Wansophark and Pramote Dechaumphai

Mechanical Engineering Department, Chulalongkorn University,  
Patumwan, Bangkok 10330, Thailand,  
Tel: 02-218-6589, Fax: 02-218-6589, E-mail: niphon.w@eng.chula.ac.th

## Abstract

A streamline upwind finite element method for 6-node triangular elements using a segregated finite element algorithm is developed. An integrated fluid-thermal-structural analysis is presented, where heat conduction in a solid is coupled with heat convection in viscous fluid flow inducing the stress in solid. The streamline upwind finite element method is used for the analysis of viscous thermal flow in the fluid region, while the analyses of heat conduction and thermal stress in solid region are performed by the Galerkin method. The solution algorithm presented in this paper uses equal order element interpolation functions for the velocities, pressure, temperature and solid displacements that can reduce the complexity in deriving the finite element equations. A segregated solution algorithm is also incorporated to compute the velocities, pressure and temperature separately for improving the computational efficiency. In addition, the adaptive meshing technique is applied to increase the analysis solution accuracy. A corresponding finite element computer program was developed and verified using simple examples that have exact solutions before applying to solve more complex problems. The computational results from several tested problems illustrate the effectiveness of the presented finite element method that can accurately predict the integrated fluid-thermal-structural phenomena.

**Keywords:** Fluid, Thermal, Structural, Finite Element Method, Adaptive Meshing Technique

## 1. Introduction

Integrated fluid-thermal-structural analysis can be founded in many engineering applications such as thermal insulation design, heat exchanger, cooling of electronic devices, solar equipment, etc. These applications are dealing with heat conduction in solid coupled with heat convection in viscous fluid flow as well as thermal stress in solid. Thus, the numerical simulation in this research area must compute the problems of solid mechanics, fluid mechanics and heat transfer simultaneously. However, most of the papers in the past still consider only two from three of these fields

such as fluid-thermal problems [1] (conjugate heat transfer problems) or fluid-solid problems [2].

In this paper, the finite element method for integrated fluid-thermal-structural analysis is presented. The 6-node triangular element is selected to produce higher-order solution accuracy of the computational algorithm. The streamline upwind finite element method for 6-node triangular element [3] is used to compute the convection term in both momentum and energy equations while the standard Galerkin method is applied for heat conduction and thermal stress in solid. The triangular elements are employed in order to combine effectively with the adaptive meshing technique presented herein. Finally, the finite element algorithm and the computer program have been verified using several examples that have the prior numerical solutions.

## 2. Theoretical formulation and solution procedure

### 2.1 Governing equations

The governing equations for integrated fluid-thermal-structural problems consist of the conservation of mass or the continuity equation, the conservation of momentum in  $x$  and  $y$  directions, the conservation of energy and the equilibrium equation.

Continuity equation,

$$\frac{\partial u}{\partial x} + \frac{\partial v}{\partial y} = 0 \quad (1a)$$

Momentum equations,

$$\rho \left( u \frac{\partial u}{\partial x} + v \frac{\partial u}{\partial y} \right) = -\frac{\partial p}{\partial x} + \mu \left( \frac{\partial^2 u}{\partial x^2} + \frac{\partial^2 u}{\partial y^2} \right) \quad (1b)$$

$$\rho \left( u \frac{\partial v}{\partial x} + v \frac{\partial v}{\partial y} \right) = -\frac{\partial p}{\partial y} + \mu \left( \frac{\partial^2 v}{\partial x^2} + \frac{\partial^2 v}{\partial y^2} \right) + \rho f_y \quad (1c)$$

where  $f_y = -g[1 - \beta(T - T_0)]$

Energy equation,

$$\rho c \left( u \frac{\partial T}{\partial x} + v \frac{\partial T}{\partial y} \right) = k \left( \frac{\partial^2 T}{\partial x^2} + \frac{\partial^2 T}{\partial y^2} \right) + \rho Q \quad (1d)$$

Equilibrium equations,

$$\frac{\partial \sigma_x}{\partial x} + \frac{\partial \tau_{xy}}{\partial y} = 0 \quad (1e)$$

$$\frac{\partial \tau_{xy}}{\partial x} + \frac{\partial \sigma_y}{\partial y} = 0 \quad (1f)$$

where  $u$  and  $v$  are the velocity components in the  $x$  and  $y$  direction, respectively;  $\rho$  is the density,  $p$  is the pressure,  $\mu$  is the viscosity,  $g$  is the gravitational acceleration constant,  $\beta$  is the volumetric coefficient of thermal expansion,  $T$  is the temperature,  $T_o$  is the reference temperature for which buoyant force in the  $y$ -direction vanishes,  $c$  is specific heat,  $k$  is the coefficient of thermal conductivity,  $Q$  is the internal heat generation rate per unit volume,  $\sigma_x$  and  $\sigma_y$  are the normal stress in  $x$  and  $y$  direction, respectively and  $\tau_{xy}$  is the shear stress. Equation (1d) can also be used for solving heat conduction in solid by setting both velocity components,  $u$  and  $v$ , as zero.

For plane strain, the relation between stress and strain is expressed by Hook's law [4] as,

$$\begin{Bmatrix} \sigma_x \\ \sigma_y \\ \tau_{xy} \end{Bmatrix} = \frac{E}{(1+\nu)(1-2\nu)} \begin{bmatrix} 1-\nu & \nu & 0 \\ \nu & 1-\nu & 0 \\ 0 & 0 & \frac{1-2\nu}{2} \end{bmatrix} \begin{Bmatrix} \varepsilon_x - \alpha(T-T_o) \\ \varepsilon_y - \alpha(T-T_o) \\ \gamma_{xy} \end{Bmatrix} \quad (2a)$$

The relation between strain and solid's displacement are

$$\varepsilon_x = \frac{\partial u_s}{\partial x}; \quad \varepsilon_y = \frac{\partial v_s}{\partial y} \quad (2b)$$

$$\gamma_{xy} = \frac{\partial u_s}{\partial y} + \frac{\partial v_s}{\partial x} \quad (2c)$$

where  $u_s$  and  $v_s$  are the solid's displacement in  $x$  and  $y$  direction, respectively.

## 2.2 Finite element formulation

The six-node triangular element is used in this study. The element assumes quadratic interpolation for the velocity components, the pressure, the temperature and the solid's displacement as

$$u(x, y) = N_i u_i \quad (3a)$$

$$v(x, y) = N_i v_i \quad (3b)$$

$$p(x, y) = N_i p_i \quad (3c)$$

$$T(x, y) = N_i T_i \quad (3d)$$

$$u_s(x, y) = N_i u_{si} \quad (3e)$$

$$v_s(x, y) = N_i v_{si} \quad (3f)$$

where  $i = 1, 2, 3, \dots, 6$ ; and  $N_i$  is the interpolation function.

The solution algorithm in this paper use the two momentum equations for solving both of the velocity components, use the combination between the continuity and the momentum equations for solving pressure, use the energy equation for solving the temperature in the solid and fluid regions, and use the equilibrium equation for solving the displacement in solid. The finite element equations corresponding to the momentum, the energy, the continuity, and the equilibrium equations are presented in the next section.

### 2.2.1 Discretization of the momentum equations

The two momentum equations, Eqs.(1b-c), are discretized using method of weighted residuals [5]. However, a special treatment of the convection terms is incorporated. These terms are approximated by a monotone streamline upwind formulation for 6-node triangular elements [3]. The method calculates the convection term directly along the streamline direction.

Using the method of weighted residuals, each momentum equation is multiplied by weighting function,  $N_i$ , and then the diffusion terms are integrated by parts using the Gauss theorem to yield the element equations in the form

$$[A]\{u\} = \{R_{px}\} + \{R_u\} \quad (4a)$$

$$[A]\{v\} = \{R_{py}\} + \{R_v\} + \{R_b\} \quad (4b)$$

where the coefficient matrix  $[A]$  contains the known contributions from the convection and diffusion terms. Further details of each matrix can be found in [6]. These element equations are assembled to yield the global equations for the velocity components. Such global equations are modified for specified velocities along the boundary prior to solving for the new velocity components.

### 2.2.2 Discretization of pressure equation

To derive the discretized pressure equation, the method of weighted residuals is applied to the continuity equation (1a). As mentioned earlier, the continuity equation is used for solving the pressure, but the pressure term does not appear in the continuity equation. For this reason, the relation between velocities and pressure are thus required. Such relations can be derived from the momentum equations (4a-b) as

$$A_{ii} u_i = - \sum_{j \neq i} A_{ij} u_j + f_i^u - \int_{\Omega} N_i \frac{\partial p}{\partial x} d\Omega \quad (5a)$$

$$A_{ii} v_i = - \sum_{j \neq i} A_{ij} v_j + f_i^v - \int_{\Omega} N_i \frac{\partial p}{\partial y} d\Omega \quad (5b)$$

where  $f_i^u$  and  $f_i^v$  are the surface integral terms and the source term due to buoyancy.

By applying the relation between velocities and pressure into the continuity equation, the pressure equation can be written in matrix form as

$$[K_p]\{p\} = \{F_u\} + \{F_v\} + \{F_b\} \quad (6)$$

The details of each matrix can be found in [6]. These element pressure equations are assembled to form the global equations, boundary conditions for the specified nodal pressures are imposed prior to solving for the updated nodal pressures.

### 2.2.3 Discretization of energy equation

The energy equation is derived using an approach which similar to the momentum equations. The streamline upwind method is applied to the convection term in the energy equation. The standard Galerkin method is then applied to yield the element equations which can be written in matrix form as

$$[K]\{T\} = \{R\} \quad (7)$$

where the matrix  $[K]$  consists of the contributions from the convection and diffusion terms. These element equations are again assembled to yield the global temperature equations. Appropriate boundary conditions are applied prior to solving for the new temperature values.

### 2.2.4 Discretization of equilibrium equation

The method of weighted residuals is applied to equation (1e-f) in the same fashion as in the momentum equations. The finite element equation can also be derived in the form

$$[K_s]\{U_s\} = \{R_s\} + \{R_T\} \quad (8)$$

where  $[K_s]$  is the stiffness matrix,  $\{U_s\}$  is the nodal displacement vector,  $\{R_s\}$  is the external load vector, and  $\{R_T\}$  is the thermal load vector. These matrices are defined by

$$[K] = \int_{\Omega} [B]^T [C] [B] d\Omega \quad (9a)$$

$$[R_s] = \int_{\Gamma} [N]^T [F_s] d\Gamma \quad (9b)$$

$$[R_s] = \int_{\Omega} [B]^T [C] \{\alpha\} (T - T_o) d\Omega \quad (9c)$$

where  $[B]$  is the strain-displacement interpolation matrix,  $[C]$  is the elastic modulus matrix,  $\{F_s\}$  is the surface traction matrix,  $\{\alpha\}$  is the thermal expansion coefficient vector,  $T_o$  is the reference temperature for zero stress state,  $\Omega$  is the element domain, and  $\Gamma$  is the element boundary.

### 2.2.5 Computational procedure

The computational procedure starts from assuming a set of initial nodal velocities, pressures, and temperatures. The new nodal temperatures in both fluid and solid region are computed using Eq. (7). The new nodal velocities and pressures are then computed using Eqs. (4a-b) and Eq. (6), respectively. The nodal velocities are then updated using Eqs. (5a-b) with the computed nodal pressures. This process is continued until the specified convergence criterion is met. The computational result of the solid temperature and the fluid pressure are then used to predict the solid deformation and stresses by equilibrium equation, Eq. (8). Such segregated solution procedure helps reducing the computer storage because the equations for the velocity components, the pressure, the temperature, and the solid displacement are solved separately.

### 3. Adaptive meshing technique

The idea behind the adaptive meshing technique presented herein is to construct a new mesh based on the solution obtained from the previous mesh. The new mesh will consist of small elements in the regions with large change in solution gradients and large elements in the other regions where the change in solution gradients is small. To determine proper element sizes at different locations in the flow field, the solid-mechanics concept for determining the principal stresses from a given state of stresses at a point is employed. Since small elements are needed in the regions of complex transport behavior, thus the distribution of quantity being transported,  $\phi$ , can be used as an indicator in the determination of proper element sizes.

To determine proper element sizes, the second derivatives of the quantity being transported with respect to the global coordinates  $x$  and  $y$  are first computed,

$$\begin{bmatrix} \frac{\partial^2 \phi}{\partial x^2} & \frac{\partial^2 \phi}{\partial x \partial y} \\ \frac{\partial^2 \phi}{\partial x \partial y} & \frac{\partial^2 \phi}{\partial y^2} \end{bmatrix} \quad (10)$$

The principal quantities in the principal directions  $X$  and  $Y$  where the cross derivatives vanish, are then determined,

$$\begin{bmatrix} \frac{\partial^2 \phi}{\partial X^2} & 0 \\ 0 & \frac{\partial^2 \phi}{\partial Y^2} \end{bmatrix} \quad (11)$$

The magnitude of the larger principal quantity is then selected,

$$\lambda = \max \left( \left| \frac{\partial^2 \phi}{\partial X^2} \right|, \left| \frac{\partial^2 \phi}{\partial Y^2} \right| \right) \quad (12)$$

This value is used to compute proper element size  $h$  at that locations from the conditions,

$$h^2 \lambda = \text{constant} = h_{\min}^2 \lambda_{\max} \quad (13)$$

where  $h_{\min}$  is the specified minimum element size, and  $\lambda_{\max}$  is the maximum principal quantity for the entire model.

Based on the condition shown in Eq. (13), proper element sizes are generated according to the given minimum element size  $h_{\min}$ . Specifying too small  $h_{\min}$  may result in a model with an excessive number of elements. On the other hand, specifying too large  $h_{\min}$  may result inadequate solution accuracy or excessive analysis and remeshing cycles. These factors must be considered prior to generating a new mesh.

#### 4. Results

The conjugate natural convection in a square cavity with a conducting wall is selected to evaluate the finite element formulation. Then the performance of the adaptive meshing technique for integrated fluid-thermal-structural analysis is evaluated by the problem of flow past three heated fins.

#### 4.1 Conjugate natural convection in a square cavity with a conducting wall

The first example for evaluate the presented schemes is the conjugate natural convection in a square cavity with a conducting wall as shown in Fig. 1. The fluid in the cavity is heated from the higher temperature solid wall along the left side and maintained at zero temperature along the right side, all other boundaries are insulated. Figure 2 shows the finite element model for both the solid wall and the fluid region consisting of 7,857 nodes and 3,840 triangles. The predicted streamline and temperature contours for the different thermal conductivity ratios  $K = k_s/k_f = 1$  and 10 at the Grashof numbers of  $10^3$  and  $10^5$  are shown in Figs. 3 and 4, respectively. The thermal conductivity ratio is defined as the thermal conductivity of solid,  $k_s$ , divided by the thermal conductivity of fluid,  $k_f$ . Figure 5(a) and (b) show the temperature and the heat flux distributions along the solid-fluid interface, respectively, with the variation of conduction ratio,  $K$ . In addition, Table 1 compares the predicted average Nusselt numbers along the interface,  $\overline{Nu}_{x=0.2}$ , with the results using the boundary-domain integral method by Hriberšek [7]. The table shows good agreement of the average Nusselt numbers for both the temperature and the heat flux.

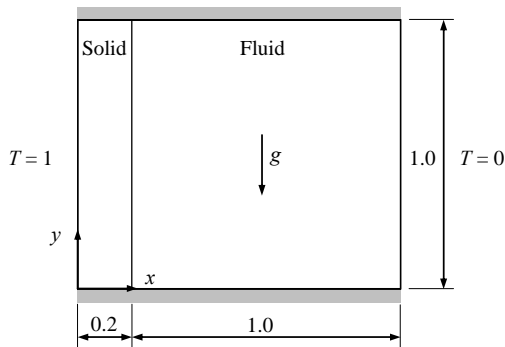


Fig. 1 Conjugate natural convection problem.

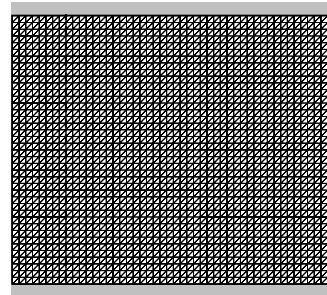


Fig. 2 Finite element model for the conjugate natural convection problem.

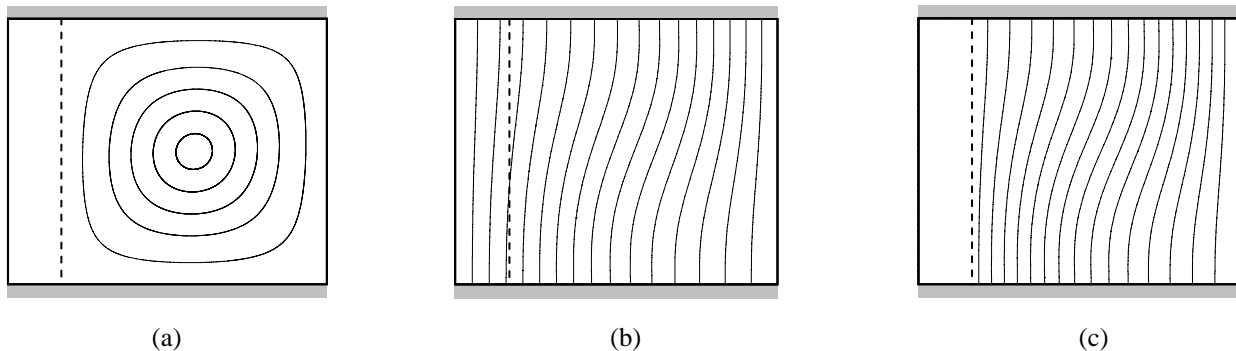


Fig. 3 (a) Streamline contours for  $K = 10$ , (b) Temperature contours for  $K = 1$  and (c) Temperature contours for  $K = 10$ , all at  $Gr = 10^3$ .

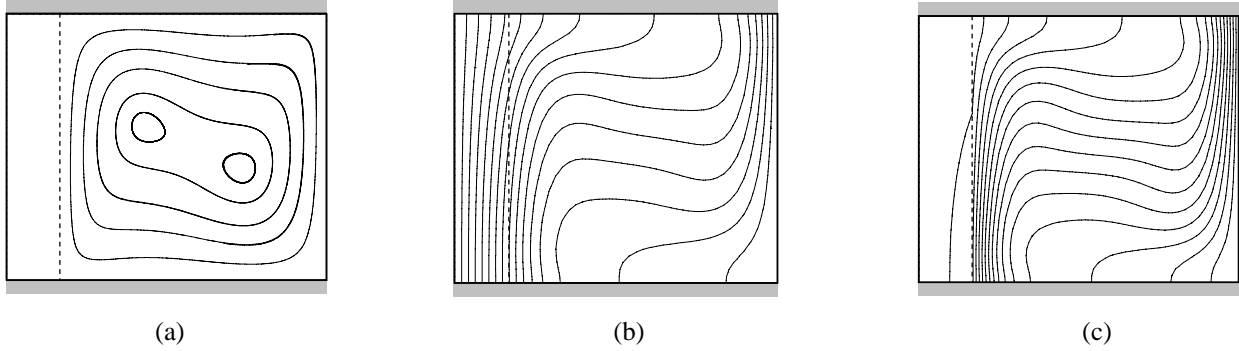


Fig. 4 (a) Streamline contours for  $K = 10$ , (b) Temperature contours for  $K = 1$  and (c) Temperature contours for  $K = 10$ , all at  $Gr = 10^5$ .

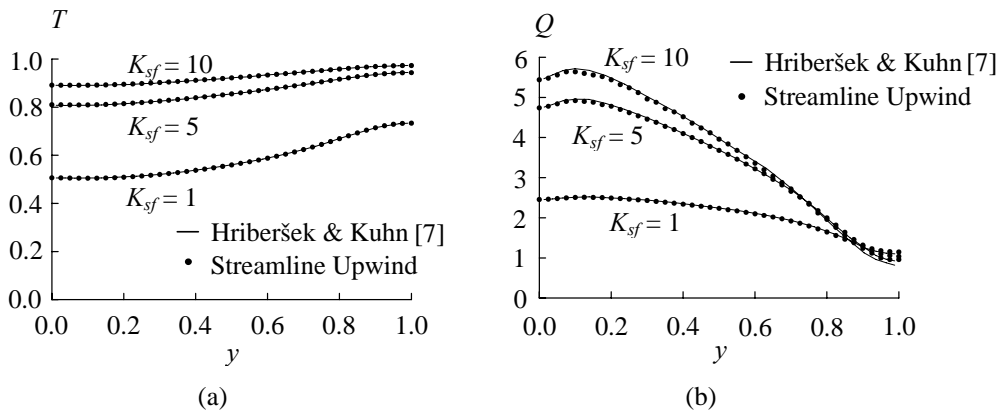


Fig. 5 (a) Interface temperatures and (b) Interface heat fluxes, all at  $Gr = 10^5$ .

Table 1 Variation of the average Nusselt numbers along interface (% difference from Ref. [7]).

Gr	conductivity ratio, $K$	1	5	10
$10^5$	Hriberšek [7]	2.08	3.42	3.72
$10^5$	Presented method	2.04 (1.92%)	3.31 (3.22%)	3.60 (3.23%)

#### 4.2 Flow past three heated fins

The problem statement of the second example as shown in Fig. 6 consists of flow between parallel plates with three heated fins where the fluid enters with a fully developed profile from the left side and leaves at the right side of the computational domain. The adaptive finite element method starts from creating a relatively uniform mesh as shown in Fig. 7. The initial mesh consists of 4,715 nodes and 2,260 elements. The figure also shows the predicted temperature contours.

The numerical solution obtained from the initial mesh is then used to construct the second adaptive mesh as describe in section 3. The second adaptive mesh and the predicted temperature contours are shown in Fig. 8. The figure shows smaller elements are generated in the region near the fin surfaces where large change in temperature gradients occurs.

The entire process is repeated again to generate the third adaptive mesh and the predicted temperature results as shown in Fig. 9. Figure 10 shows the comparisons of the temperature distribution along the fin's surfaces with the numerical results from Davalath and Bayazitoglu [8]. The figure shows the adaptive mesh provides higher solution accuracy compared to the results from the initial mesh because small elements are generated automatically in the regions of complex flow behavior. After that, the temperature distribution in fins and pressure distribution along the fin's surfaces are applied as boundary condition for thermal stress analysis of the fins. Figure 11 shows the Von Mises stress and vector of displacement of fins.

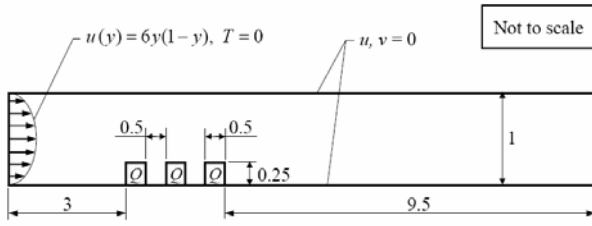


Fig. 6 Problem statement of flow past three fins.

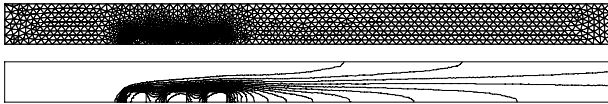


Fig. 7 Initial mesh and temperature distributions.

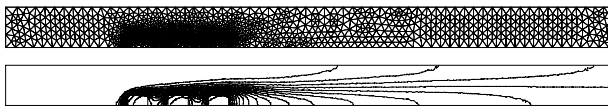


Fig. 8 The second adaptive mesh and temperature distributions.

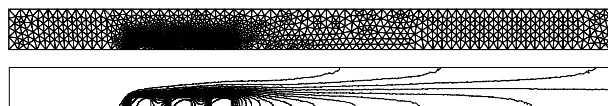


Fig. 9 The third adaptive mesh and temperature distributions.

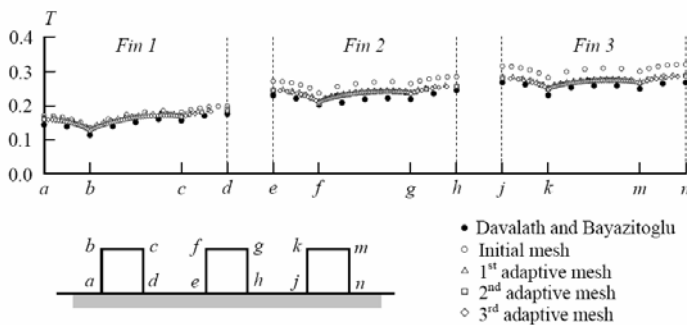


Fig. 10 Comparison of numerical results of the initial and the adaptive mesh.

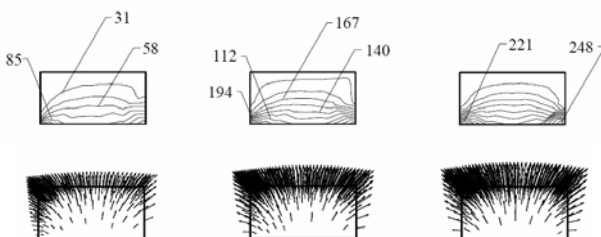


Fig. 11 Von Mises stress and vector of displacement of fins.

## 5. Conclusion

The integrated fluid-thermal-structural analysis was presented. The method combines the viscous thermal flow analysis of the fluid region and the heat transfer analysis in the solid region together. The streamline upwind finite element method for 6-node triangular element was used to evaluate the convection term in both momentum and energy equations. The flow analysis used a segregated solution algorithm to compute the velocities, the pressure and the temperature separately for improving the computational efficiency. The standard Galerkin method was used to predict the stress distribution in solid region. The finite element formulation, the computational procedure and the basic behind the adaptive meshing technique were described. The efficiency of the coupled finite element method has been evaluated by several examples that were previously performed using other methods. These examples demonstrate the capability of the proposed formulation for integrated fluid-thermal-structural analysis.

## Acknowledgements

The authors are pleased to acknowledge the Thailand Research Fund (TRF) for supporting this research work.

## References

- [1] Malatip, A., Wansoaphark, N., and Dechaumphai, P., 2006. Combined Streamline Upwind Petrove Galerkin Method and Segregated Finite Element Algorithm for Conjugate Heat Transfer Problems. *Journal of Mechanical Science and Technology (KSME int. J.)*, Vol. 20, No. 10, pp. 1741-1752.
- [2] Sarrate, J., Huerta, A., and Donea, J., 2001. Arbitrary Lagrangian-Eulerian formulation for fluid-rigid body interaction. *Comput. Methods Appl. Mech. Engrg.*, Vol.190, pp. 3171-3188.
- [3] Wansoaphark, N., and Dechaumphai, P., 2006. Adaptive Streamline Upwind Finite Element Method Using 6-node Triangular Element for Analyzing Convective-Diffusion Problem. 20<sup>th</sup> Conference of Mechanical Engineering Network of Thailand, Nakhon Ratchasima, Thailand, October 18-20.
- [4] Beer, F.P., Johnston, E.R., and DeWolf, J.T., 2002, *Mechanics of Materials*, Third Edition, New York: McGraw-Hill.
- [5] Dechaumphai, P. 2007, *Finite Element Method in Engineering*, Chulalongkorn University Press, Bangkok.
- [6] Wansoaphark, N. 2007, *Adaptive Streamline Upwind Finite Element for Integrated Fluid-Thermal-Structural Analysis*, Ph.D. Dissertation, Chulalongkorn University, Bangkok.
- [7] Hriberšek, M. and Kuhn, G., 2000. Conjugate Heat Transfer by Boundary-Domain Integral Method. *Engineering Analysis with Boundary Elements*, Vol. 24, pp. 297-305.
- [8] Davalath, J., and Bayazitoglu, Y., 1987. Forced Convection Cooling Across Rectangular Blocks. *Journal of Heat Transfer*, Vol.109, pp. 321-328.